Cell Reports

CDK1-PP2A-B55 interplay ensures cell cycle oscillation via Apc1-loop^{300}

Graphical abstract

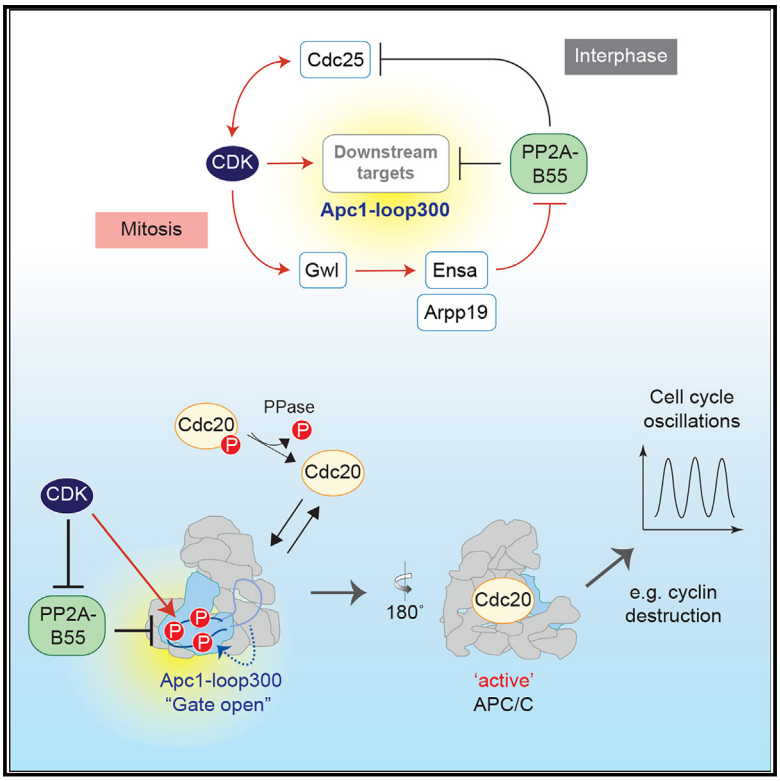

Highlights

- PP2A-B55 opposes CDK1 by dephosphorylating the Apc1-loop^{300} domain on the APC/C
- Premature activation of PP2A-B55 during mitosis stalls APC/C activity
- Cdc20 dynamically interacts with mitotic APC/C, essential for its activation
- Dephosphorylated Apc1-loop^{300} domain prevents dynamic association of Cdc20 to APC/C

Authors

Kim Hou Chia, Hiroko Takaki, Kazuyuki Fujimitsu, Sarah Darling, Juan Zou, Juri Rappsilber, Hiroyuki Yamano

Correspondence

h.yamano@ucl.ac.uk

In brief

Chia et al. reveal PP2A-B55's crucial role in APC/C phospho-regulation, showing that its mitotic activation leads to APC/C inactivation by blocking Cdc20's binding via Apc1-loop^{300} dephosphorylation. This discovery emphasizes the CDK-PP2A axis's pivotal role in controlling cell cycle oscillation through APC/C regulation.

Chia et al., 2024, Cell Reports *43*, 114155
May 28, 2024
https://doi.org/10.1016/j.celrep.2024.114155

Cell Reports

CellPress
OPEN ACCESS

Report

CDK1-PP2A-B55 interplay ensures cell cycle oscillation via Apc1-loop^{300}

Kim Hou Chia,[1] Hiroko Takaki,[1] Kazuyuki Fujimitsu,[1] Sarah Darling,[1] Juan Zou,[2] Juri Rappsilber,[2,3] and Hiroyuki Yamano[1,4,*]

[1]Cell Cycle Control Group, University College London (UCL) Cancer Institute, London WC1E 6DD, UK
[2]University of Edinburgh, Wellcome Centre for Cell Biology, Edinburgh EH9 3BF, UK
[3]Technische Universität Berlin, Chair of Bioanalytics, 10623 Berlin, Germany
[4]Lead contact
*Correspondence: h.yamano@ucl.ac.uk
https://doi.org/10.1016/j.celrep.2024.114155

SUMMARY

Cell cycle control relies on a delicate balance of phosphorylation with CDK1 and phosphatases like PP1 and PP2A-B55. Yet, identifying the primary substrate responsible for cell cycle oscillations remains a challenge. We uncover the pivotal role of phospho-regulation in the anaphase-promoting complex/cyclosome (APC/C), particularly through the Apc1-loop^{300} domain (Apc1-300L), orchestrated by CDK1 and PP2A-B55. Premature activation of PP2A-B55 during mitosis, induced by Greatwall kinase depletion, leads to Apc1-300L dephosphorylation, stalling APC/C activity and delaying Cyclin B degradation. This effect can be counteracted using the B55-specific inhibitor pEnsa or by removing Apc1-300L. We also show Cdc20's dynamic APC/C interaction across cell cycle stages, but dephosphorylation of Apc1-300L specifically inhibits further Cdc20 recruitment. Our study underscores APC/C's central role in cell cycle oscillation, identifying it as a primary substrate regulated by the CDK-PP2A partnership.

INTRODUCTION

The cell cycle, an essential process for life, orchestrates the accurate duplication and segregation of DNA into daughter cells. This complex mechanism not only ensures genetic continuity through meiosis and mitosis but also regulates cellular growth, proliferation, and differentiation, responding to environmental signals to maintain genomic stability. At the core of this regulation are cyclin-dependent kinases (CDKs), phosphatases such as PP1 and PP2A-B55, and the anaphase-promoting complex/cyclosome (APC/C).[1–8] CDK1, a primary kinase in the cell cycle, is crucial for initiating mitosis.[2,9,10] Concurrently, in recent decades, phosphatase activities, such as PP1 and PP2A-B55, have emerged as important players in cell cycle progression.[11–14] Among them, PP2A-B55 has been highlighted as a key counterbalance to CDK1. The delicate equilibrium between CDK1 and PP2A-B55 activities is critical for proper cell cycle progression. For instance, elevated PP2A-B55 activity can inhibit mitotic entry, while its removal leads to premature mitotic initiation in *Xenopus* egg extracts.[11] Despite our understanding of the roles of CDK1 and PP2A-B55, the primary substrates dictating cell cycle oscillation and their regulatory molecular mechanisms are still elusive, posing a significant challenge in the field.

The APC/C, an unusually large E3 ubiquitin ligase, governs the cell cycle through ubiquitin-mediated proteolysis and is activated by either Cdc20 or Cdh1 as its co-activator.[4–8] This complex regulates the degradation of specific proteins at defined stages, ensuring orderly mitotic progression. One of its primary roles involves the degradation of securin and Cyclin B, which are essential for sister chromatid separation and mitotic exit. Post-translational modifications, especially phosphorylation, play a central role in APC/C regulation. We and others have shown the key role of CDK1 in activating the APC/C, particularly in initiating the degradation of Cyclin B. This action of CDK1, in turn, contributes to its own inactivation, ensuring cell cycle oscillation. This is achieved by CDK1's phosphorylation of specific intrinsically disordered regions in Apc3 and Apc1, specifically the Apc3-loop and Apc1-loop^{300} (hereafter called Apc1-300L), following a sequential phosphorylation relay mechanism.[15–17] Apc1-300L, encompassing roughly 100 evolutionarily conserved amino acids (294–399 in *Xenopus*), not only sterically hinders Cdc20's association with APC/C but also acts as a phosphorylation-sensitive activation switch. This highlights its pivotal role in counteracting Apc1-300L autoinhibition and facilitating Cdc20's association with the mitotic APC/C.[15–17] Notably, while phosphorylation is crucial for controlling Cdc20 recruitment, Apc1-300L dephosphorylation dynamics are poorly studied. Adding complexity to this regulation is the negative phospho-regulation of APC/C co-activators such as Cdc20, hindering APC/C association.[18,19] Phosphatases responsible for Cdc20 have been reported in some contexts,[19–23] but clearly much remains to be uncovered.

In this study, we explore the dephosphorylation mechanism of Apc1-300L, investigating its role in Cdc20 recruitment and APC/C activation. We identify critical residues for its phosphorylation-sensitive switch function and examine phosphorylation dynamics and its effects on Cdc20 interaction. Our insights

into CDK-PP2A-mediated Apc1-300L phospho-regulation underscore its crucial role in cell cycle oscillation and genetic integrity maintenance.

RESULTS

Phosphorylation modulates Apc1-300L interactions within APC/C

While we have a grasp on the roles of CDK1 and PP2A-B55, the key substrates driving cell cycle oscillations remain elusive (Figure 1A). Our initial goal was to comprehensively understand the phosphorylation dynamics of Apc1-300L and its impact on interactions within the APC/C. Using cross-linking mass spectrometry (CLMS), we examined the interaction patterns of Apc1-300L in unphosphorylated versus hyper-phosphorylated APC/C_wild type (WT) complexes. We found that hyper-phosphorylation reduces cross-links between Apc1-300L and key residues at co-activator binding sites on Apc8 and Apc6 (Figure 1B). This observation aligns with previous studies that link phosphorylation-mediated displacement of Apc1-300L to enhanced Cdc20 recruitment.[15–17] Importantly, Cdc20 requires dephosphorylation for effective APC/C-Cdc20 complex assembly,[18,19] while APC/C activation itself is dependent on phosphorylation.

Identification of the phosphatase regulating Apc1-300L dephosphorylation

We sought to uncover the mechanisms that regulate Apc1-300L de/phosphorylation throughout the cell cycle. Utilizing a pulse-chase assay, we tracked ^{32}P removal from Apc1-300L and Cdc20 in cytostatic factor (CSF)-mediated meiosis metaphase II-arrested *Xenopus* egg extracts (CSF extracts) (Figures 1C and 1D). While Cdc20-T79 quickly dephosphorylated, indicating its importance for APC/C binding affinity,[19] Apc1-300L's dephosphorylation was minimal. Inhibition of Cdc20-T79 dephosphorylation by okadaic acid[19] (Figures 1C and 1D) suggests a dormant state for Apc1-300L's phosphatase during mitosis. In contrast, PP2A and similar phosphatases actively dephosphorylate Cdc20, facilitating the formation of the APC/C-Cdc20 complex.

The primary candidate phosphatase responsible for this activity is PP2A-B55, which is known to oppose CDK functions. To investigate this mechanism, we depleted Greatwall (Gwl) kinase, which inhibits PP2A-B55 via Ensa/Arpp19 phosphorylation,[24–26] from CSF extracts and induced early PP2A-B55 activation. After Gwl depletion, rapid dephosphorylation of Apc1-300L occurred, yet the introduction of thio-phosphorylated Ensa (pEnsa), a PP2A-B55 inhibitor, ceased this process (Figures 1E and 1F). The dephosphorylation kinetics of Apc1-300L were notably fast, with a half-life of approximately 1.5 min (Figure 1G). These results confirm PP2A-B55's crucial role in Apc1-300L dephosphorylation, regulated by the Gwl-Ensa/Arpp19 pathway.

Previously, we demonstrated that the Apc1-300L-7A variant, in which all seven serine residues at the CDK phosphorylation consensus site (Figure 2A) are replaced by alanine, exhibits high affinity for the APC/C complex.[15] To identify the residues critical for Apc1-300L's association with APC/C, we conducted a binding assay using variants of Apc1-300L-6A, each preserving a single phosphorylatable serine (Figure S1A), followed by APC/C pull-down analysis. Phosphorylation at S358 or S380 significantly impaired Apc1-300L's interaction with APC/C, while modifications at S314 or S344 modestly reduced binding (Figures S1B and S1C). To monitor these phosphorylation events on endogenous APC/C in *Xenopus* egg extracts, we developed phospho-specific antibodies targeting S314/S318, S358, and T378/S380. The phosphorylation of these sites was abolished upon premature activation of PP2A-B55, and their dephosphorylation was inhibited by pEnsa or okadaic acid (Figure 2B), suggesting that PP2A-B55 dephosphorylates Apc1-300L.

Next, we investigated Apc1-300L dephosphorylation during mitotic exit. Introducing the CDK1 inhibitor p27 to anaphase extracts led to a sharp decline in Apc1-300L phosphorylation, as evidenced by ^{32}P removal (Figures S2A and S2B). This decrease was impeded by NIPP1 and pEnsa, inhibitors of PP1 and PP2A-B55, respectively, but remained unaffected by the PP2A-B56 inhibitor (B56i). Given the roles of PP1 and PP2A-B55 in counteracting CDK activity during mitotic exit[11,12,27] and PP1's potential to activate PP2A-B55 through the Gwl-Ensa/Arpp19 pathway,[24–26,28–31] we examined PP1's contribution to Apc1-300L dephosphorylation (Figure 2C). Consistent with the observations in Figure S2A, the PP1 inhibitor (NIPP1) inhibited Apc1-300L dephosphorylation, but adding pEnsa did not enhance this effect. To isolate PP1's effect, given that NIPP1 affects PP2A-B55 via Gwl, we removed Gwl kinase. Eliminating Gwl kinase negated NIPP1's impact, while pEnsa persistently blocked dephosphorylation, underscoring PP2A-B55, not PP1, as the primary phosphatase for Apc1-300L during mitotic exit. This aligns with previous findings that PP2A-B55 targets human APC1 S355, analogous to *Xenopus* Apc1 S358, for dephosphorylation during mitotic exit.[23]

Finally, by using purified proteins, we demonstrated that recombinant PP2A-B55 directly dephosphorylates Apc1-300L, highlighting its specific role in targeting this dephosphorylation. Importantly, the presence of pEnsa inhibited this activity (Figure 2D), reinforcing PP2A-B55's direct involvement in Apc1-300L dephosphorylation.

Activation of PP2A-B55 in mitosis inactivates APC/C through Apc1-300L

We propose that Apc1-300L, influenced by CDK and PP2A-B55's phospho-regulation, plays a critical role in mitotic control, acting as a central hub for signal integration to ensure orderly mitotic progression. To investigate this hypothesis, we explored the premature activation of PP2A-B55 on APC/C activity in CSF-mediated meiosis metaphase II-arrested extracts. Notably, APC/C-Cdc20 complex activation in these extracts is initially inhibited by XErp1/Emi2,[32] whose inactivation triggers anaphase onset.[33,34] We found that Cyclin B degradation, a marker of APC/C activation, occurs within 20 min after XErp1 depletion (Figure 3A, lanes 5–8). However, premature PP2A-B55 activation, by Gwl depletion (GwlΔ), blocked Cyclin B degradation (lanes 13–16), underscoring PP2A-B55's role in suppressing APC/C. Adding pEnsa to GwlΔ extracts restored Cyclin B degradation (lanes 21–24), confirming PP2A-B55's inhibitory effect on APC/C activation.

To further investigate, we monitored the degradation of ^{35}S-labelled Cyclin B and NIMA (Never in mitosis gene A)-related

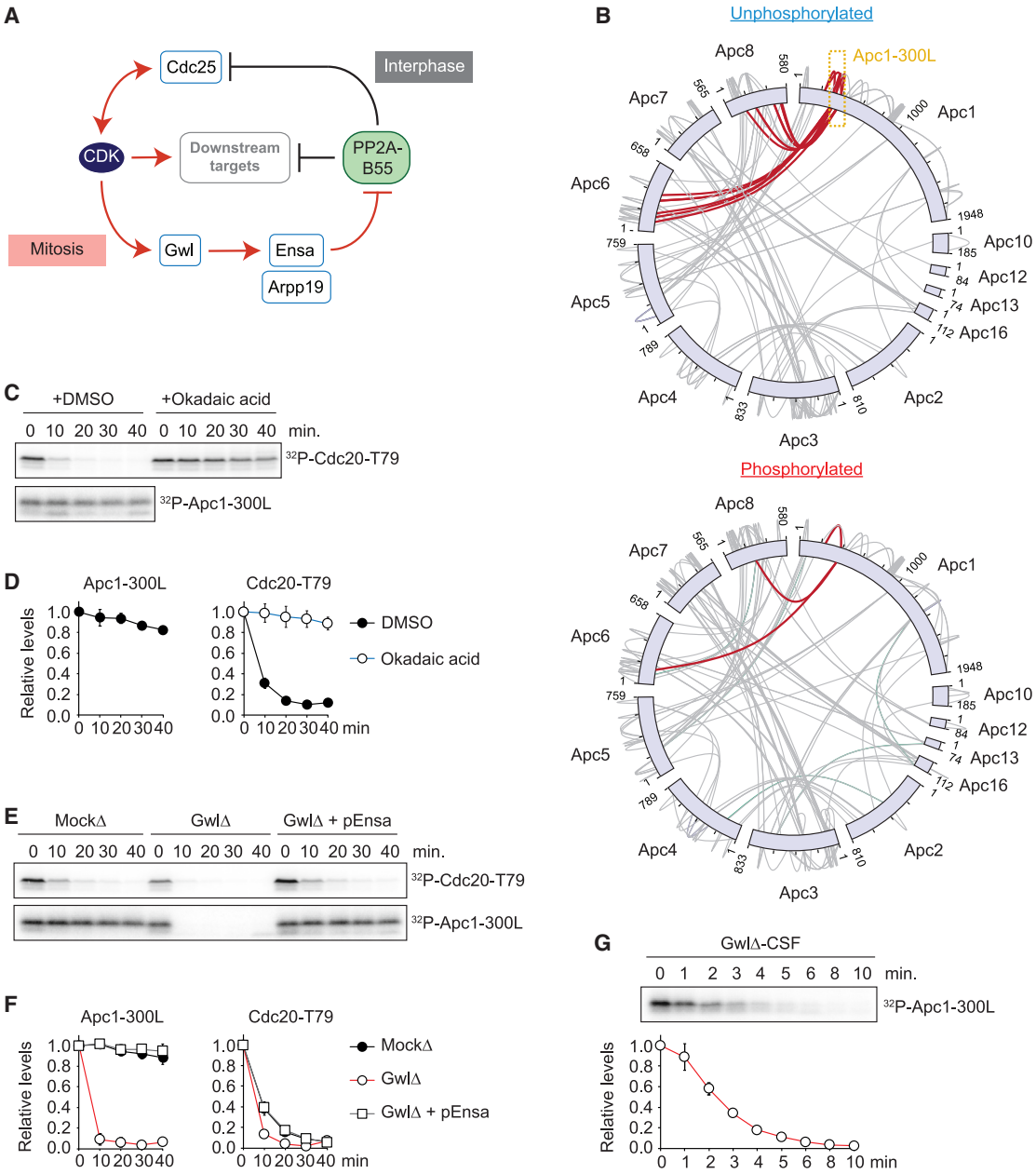

Figure 1. Apc1-300L dephosphorylation in PP2A-B55-activated *Xenopus* egg extracts

(A) Schematic depicting the mutual regulation between CDK and PP2A-B55. Downstream targets remain underexplored.

(B) Circular plots (xiVIEW) show intra- and inter-protein cross-links in rAPC/C complexes, comparing unphosphorylated (top) to hyper-phosphorylated states (bottom). Gray lines represent all Apc subunit cross-links; Apc1-300L cross-links are highlighted in red.

(C) Phosphatase assay of Cdc20 (T79) and Apc1-300L in mitosis. After phosphorylation with CDK-Cyclin A and [γ-^{32}P]-ATP, substrates were added to CSF extracts with DMSO or 2 μM okadaic acid. Samples were analyzed by SDS-PAGE and autoradiography.

(D) Quantification of (C), normalizing ^{32}P levels to initial intensities, with 0 min set to 1.0. Data represent the average of three experiments ± SEM.

(E) Phosphatase assay of Cdc20 (T79) and Apc1-300L in PP2A-B55-activated extracts. CSF extracts underwent immunodepletion using either beads (MockΔ) or Gwl antibody-bound beads (GwlΔ) at 23°C, and then either buffer or 5 μM pEnsa was added. Analysis was performed as in (C).

(F) Quantification of (E), with data from three (Cdc20) or four (Apc1-300L) experiments ± SEM and initial intensities set to 1.0.

(G) Short-interval Apc1-300L dephosphorylation by PP2A-B55, following the procedure in (E) and quantified as in (F).

kinase 2A (Nek2A) in anaphase extracts via a destruction assay (Figures 3B and 3C). As observed in CSF extracts, activating PP2A-B55 significantly reduced both substrates' degradation, an effect reversed by pEnsa, suggesting PP2A-B55's APC/C inactivation role. We then examined PP2A-B55's impact on APC/C via Apc1-300L using a recombinant APC/C (rAPC/C)

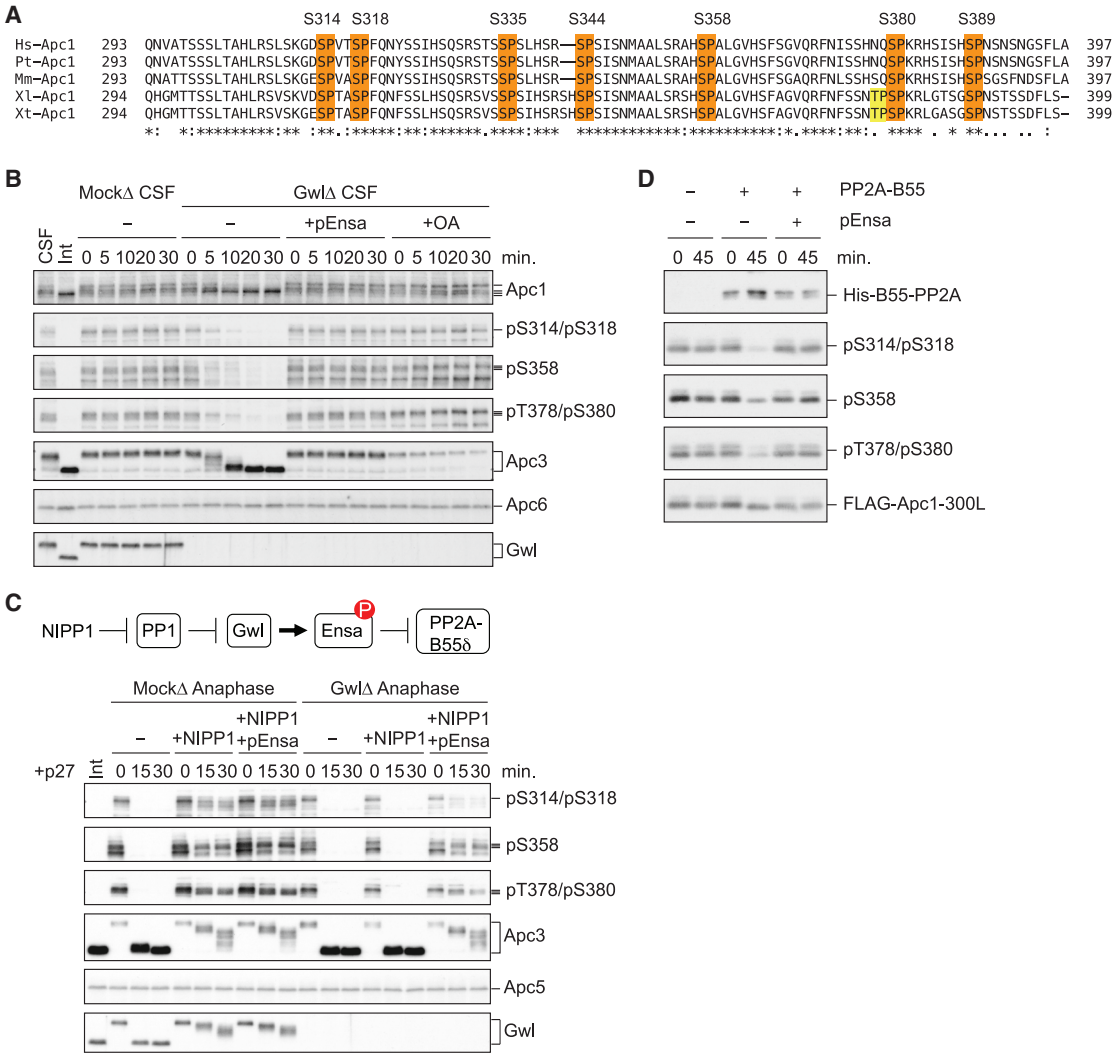

Figure 2. Apc1-300L dephosphorylation by PP2A-B55, not PP1, in *Xenopus* egg extracts

(A) Multiple alignment of Apc1-300L sequences from various species (Hs, *Homo sapiens*; Pt, *Pan troglodytes*; Mm, *Mus musculus*; Xl, *Xenopus laevis*; Xt, *Xenopus tropicalis*), with the CDK phosphorylation site highlighted in yellow and orange. Conserved amino acids are marked with asterisks, while similar ones are denoted by colons and dots.

(B) Investigation of endogenous Apc1-300L phosphorylation status in PP2A-B55 activated CSF extracts. Beads (MockΔ) or Gwl antibody-bound beads (GwlΔ) were mixed with CSF extracts at 23°C for 20 min. Before recovering the immunodepleted extracts, either buffer, 5 μM pEnsa or 2 μM okadaic acid was introduced. Samples taken at the indicated time points were analyzed by SDS-PAGE and immunoblotting.

(C) Comparison of Apc1-300L dephosphorylation by PP2A-B55 against PP1, using methods from (B) with added NIPP1 (12 μM) and pEnsa (5 μM) and then p27 to induce mitotic exit.

(D) *In vitro* phosphatase assay using phosphorylated Apc1-300L and purified PP2A-B55. Post CDK-Cyclin A phosphorylation, Apc1-300L was incubated with mock or PP2A-B55, with/without 10 μM pEnsa, and analyzed by SDS-PAGE and immunoblotting.

mutant without Apc1-300L (Apc1-300LΔ) and WT rAPC/C in anaphase extracts (Figures 3D and S3A–S3C). While WT rAPC/C showed expected activity, PP2A-B55 activation significantly lowered it, mirroring endogenous APC/C behavior (Figure 3C). Notably, removing the Apc1-300L "autoinhibitory loop" made rAPC/C (Apc1-300LΔ) largely immune to PP2A-B55's inhibitory effects (Figure 3D), highlighting the role of Apc1-300L in PP2A-B55 mediated APC/C suppression.

To investigate the changes in Cdc20's association dynamics and APC/C activity following PP2A-B55 activation, we performed an *in vitro* ubiquitylation and Cdc20 binding assay (Figure 3E). We detected an immediate increase in Cdc20 associated with APC/C after PP2A-B55 activation in CSF extracts, peaking within 15 min before decreasing (Figure 3E, center and bottom panels). This transient increase likely results from PP2A-B55 selectively targeting phospho-threonine residues on Cdc20 over phospho-serine sites on Apc1-300L,[23,35,36] as supported by experiments conducted at earlier time points after Gwl depletion (Figure S3D). While the mechanisms behind the subsequent decline in APC/C-bound Cdc20 remain

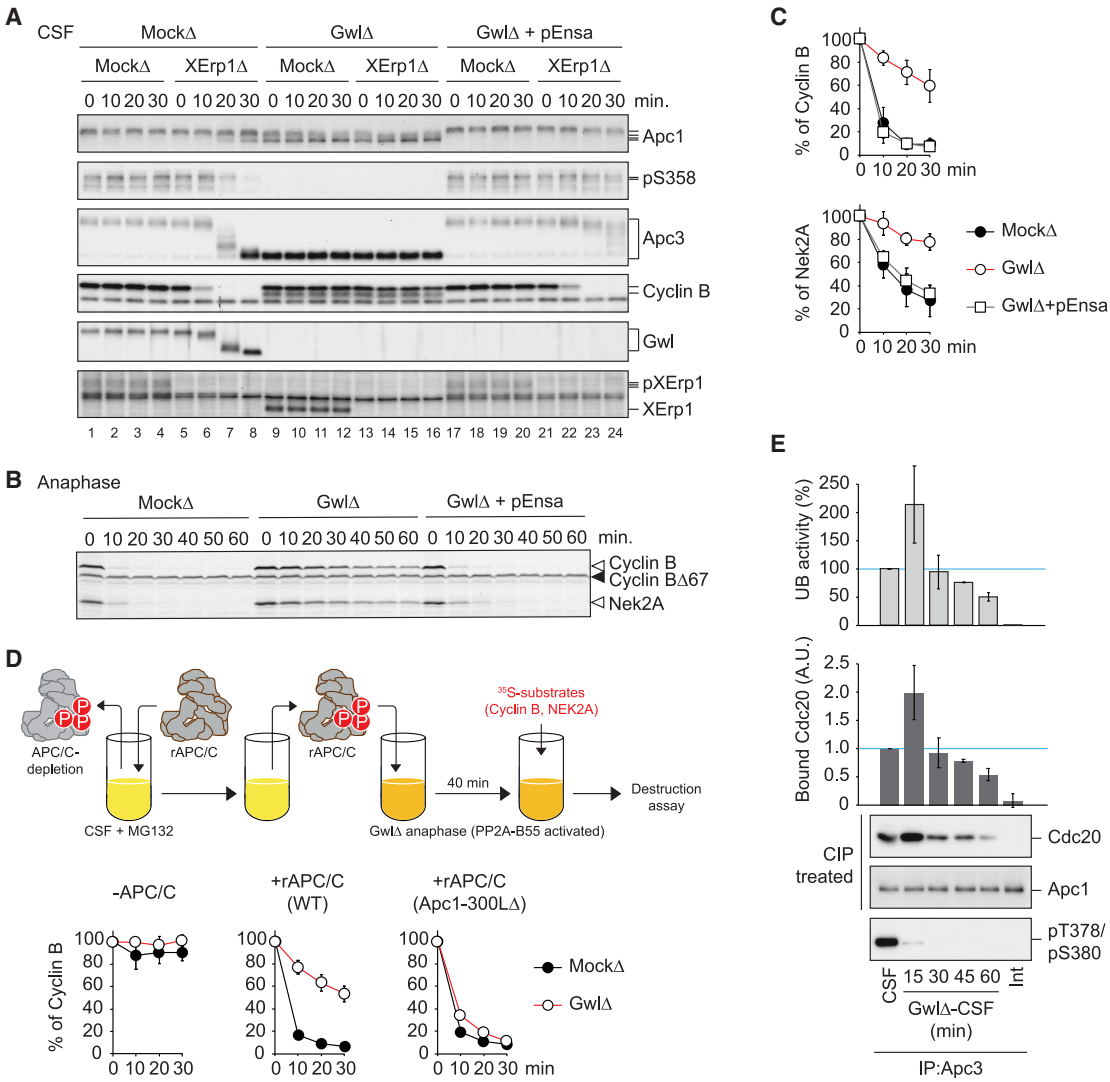

Figure 3. PP2A-B55 activation during mitosis deactivates APC/C via Apc1-300L

(A) Cyclin B degradation was evaluated following premature PP2A-B55 activation or with 5 μM pEnsa (see Figure 2B for details). Samples post immunodepletion using XErp1 antibody-bound (XErp1Δ) or unbound (MockΔ) beads were analyzed by SDS-PAGE and immunoblotting.

(B) Premature PP2A-B55 activation affects APC/C substrate degradation. ^{35}S-labeled Nek2A, Cyclin B, and Cyclin BΔ67 (stable control) tested in mock- or Gwl-depleted extracts with or without 5 μM pEnsa were analyzed by SDS-PAGE and autoradiography at the indicated times.

(C) Quantitative analysis of (B), with data means (±SEM) from three experiments. Intensities at 0 min were set to 1.0.

(D) rAPC/C destruction assay showing Apc1-300L's involvement in PP2A-B55-mediated APC/C deactivation. Top: experimental schematic. ^{35}S-labeled substrate quantification is shown (data from three experiments ± SEM). Refer to Figures S3A and S3B.

(E) *In vitro* ubiquitylation assay in the PP2A-B55-activated context. APC/C activity and Cdc20 levels were quantified post immunoprecipitation (procedure in Figure 2B), relative to CSF intensity, averaged over three trials (±SEM). See also Figure S3E.

elusive, our ubiquitylation assay shows a direct link between APC/C-Cdc20 complex activity and its Cdc20 content (Figure 3E, top chart; Figure S3E), implying that PP2A-B55 activation dampens APC/C activity.

Mechanism of PP2A-B55-mediated inactivation of APC/C

How does the dephosphorylation of Apc1-300L by PP2A-B55 influence APC/C activity? Building on findings that dephosphorylated Apc1-300L binds more strongly to APC/C,[15] as further evidenced in Figure S1, we explored its potential to displace Cdc20. Using a Cdc20 dissociation assay, we examined the dissociation behavior of Cdc20 from both WT and loop-deleted rAPC/C variants upon PP2A-B55 activation (Figures S4A–S4C). The assay employed Cdc20-5A, a CDK-insensitive mutant known for its robust binding affinity[19] and detectability via a FLAG tag, which was mixed with purified rAPC/C in extracts devoid of endogenous APC/C and Cdc20. The resultant rAPC/C-Cdc20 complex was then introduced into PP2A-B55-activated extracts lacking APC/C. Our observations of FLAG-Cdc20-5A's dissociation from both APC/C variants over time

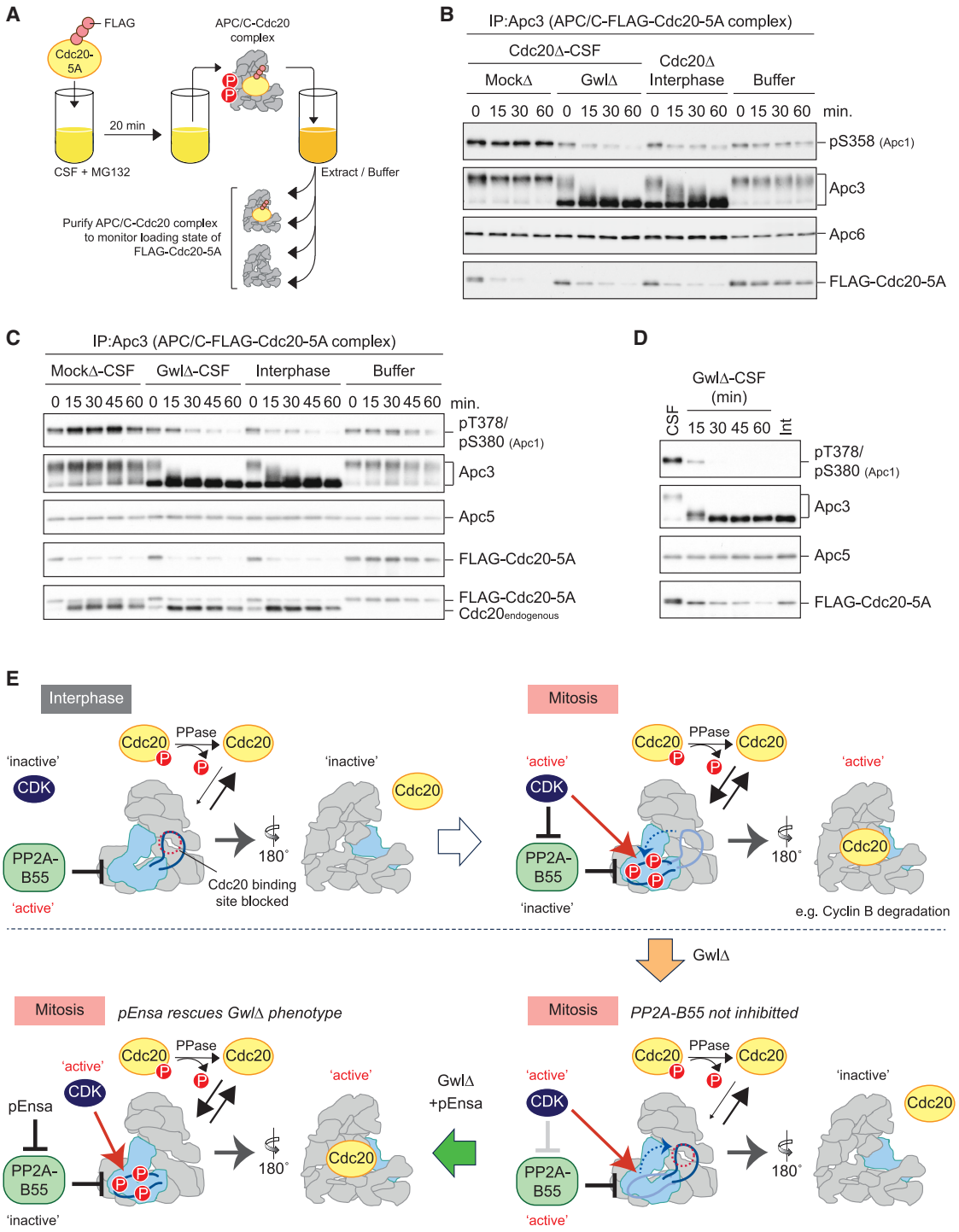

Figure 4. Impact of Apc1-300L dephosphorylation on APC/C-Cdc20 interaction

(A) Schematic of the dissociation assay.

(B) Analysis of Cdc20 dissociation from APC/C in *Xenopus* egg extracts. FLAG-Cdc20-5A was introduced into Cdc20-depleted extracts with MG132, and the APC/C-Cdc20 complex's dissociation was tested under various conditions (mock or Gwl depletion). Samples were analyzed via SDS-PAGE and immunoblotting.

(C) Dynamic reassociation of endogenous Cdc20 with APC/C in *Xenopus* egg extracts, following the approach in (B).

(D) Assays for *de novo* Cdc20 loading. Activation of PP2A-B55 lessens Cdc20's APC/C binding. After mock and Gwl depletion, extracts were supplemented with FLAG-Cdc20-5A and Apc3-bound Dynabeads, and the retrieved APC/C-Cdc20 complex was examined using SDS-PAGE and immunoblotting.

(legend continued on next page)

demonstrate that Apc1-300L does not promote Cdc20 dissociation in response to PP2A-B55 activation.

To confirm our findings, we repeated the dissociation assay with endogenous APC/C both in the presence and absence of PP2A-B55 activation (Figures 4A and 4B). Mirroring results from rAPC/C experiments, FLAG-Cdc20-5A dissociated from endogenous APC/C under all conditions, including interphase, regardless of PP2A-B55 activation, with controls (buffer) showing no separation. Dissociation also occurred for both ^{35}S-labeled Cdc20-5A without the FLAG tag and FLAG-tagged Cdh1-4A (Figures S4D and S4E), indicating that dissociation is not influenced by the FLAG tag and is consistent across both Cdc20 and Cdh1. The reassociation of endogenous Cdc20 with APC/C after FLAG-Cdc20-5A dissociation (Figure 4C, bottom) underscores the dynamic interplay between Cdc20 and APC/C in *Xenopus* egg extracts, reinforcing that Apc1-300L dephosphorylation does not facilitate Cdc20's dissociation from APC/C.

Our final experiment evaluated whether Apc1-300L dephosphorylation by PP2A-B55 acts as a "closing gate" preventing Cdc20 reassociation with the APC/C. We introduced FLAG-Cdc20-5A into PP2A-B55-activated CSF extracts at staggered time points, each for a duration of 10 min, and subsequently measured the co-purification with APC/C (Figure 4D). We observed a progressive decline in FLAG-Cdc20-5A association with APC/C concurrent with PP2A-B55 activation, suggesting that PP2A-B55 impairs Cdc20's binding to APC/C. Remarkably, adding pEnsa reversed this effect in PP2A-B55-activated extracts (Figure S4F), highlighting PP2A-B55's significant impact on Cdc20's binding efficiency. Additionally, using an rAPC/C variant devoid of Apc1-300L showed that Cdc20's association remained constant, unaffected by PP2A-B55 (Figure S4G), emphasizing Apc1-300L's key role as a gatekeeper. These results bolster our model, where PP2A-B55 regulates APC/C activity by controlling the "gate-closing" function of Apc1-300L, governing the binding of Cdc20. The re-phosphorylation of Apc1-300L "reopens" the gate, allowing Cdc20 to reassociate with the APC/C (Figure 4E).

DISCUSSION

This study elucidates the mechanism by which PP2A-B55 inactivates APC/C, advancing our understanding of the orchestration of mitotic entry and exit through the regulation of APC/C by an interplay between CDK1 and PP2A-B55. PP1 and PP2A-B55, serving as the primary phosphatases counteracting CDK1, play essential roles in dephosphorylating numerous proteins during mitotic exit. This ensures the timely separation of sister chromatids and facilitates a seamless transition out of mitosis. Our comprehensive analysis identifies Apc1-300L as a pivotal substrate for both CDK1 and PP2A-B55 (Figure 4E). Notably, Apc1-300L is exclusively dephosphorylated by PP2A-B55, not PP1, highlighting CDK1's role in inactivating PP2A-B55 via the Gwl (known as MASTL, Microtubule-associated serine/threonine kinase like, in humans) cascade during mitosis. The premature activation of PP2A-B55 could potentially compromise mitotic progression by inhibiting APC/C through the "Apc1-300L gate," affecting the dynamic interaction with Cdc20. Our CLMS findings compellingly demonstrate that phosphorylation significantly diminishes Apc1-300L's interaction with Apc8 and Apc6 (Figure 1B), underscoring a "gate" mechanism critical for APC/C activation. Governed by the CDK1-PP2A-B55 dynamic, this mechanism is crucial for precise cell cycle control, emphasizing the CDK1-PP2A-B55-APC/C axis's essential role in cell cycle regulation.

The intricate interplay between CDK1 and PP2A-B55 is fundamental to APC/C regulation. Their mutual inhibition showcases the precision with which cells manage phosphorylation events. Furthermore, the CDK-Gwl-Ensa/Arpp19 regulatory pathway serves as a protective mechanism, ensuring that PP2A-B55's phosphatase activity remains in check during essential mitotic phases (Figure 4E). Looking beyond Apc1-300L, key cell cycle transition components, such as Wee1, Cdc25, lamins, condensins, and microtubule-associated proteins, appear to be governed by the same regulatory framework. While their interactions with CDK and PP2A-B55 are recognized, their phosphorylation/dephosphorylation dynamics and substrate targets remain largely unexplored. Our study illuminates the pivotal role of Apc1 phosphorylation/dephosphorylation as a key switch in mitosis, modulated by the CDK1 and PP2A-B55 interplay. It emphasizes its critical function in cell cycle oscillation and introduces Apc1-300L as an element contributing to our understanding of cell cycle regulation, as contextualized in Figure 1A. The regulatory pattern identified for Apc1-300L may also extend to these proteins, suggesting a unified mechanism for mitotic entry, progression, and exit. In a clinical context, our findings offer potential opportunities in oncology. Targeting Gwl or its human analog, MASTL kinase, has emerged as a promising therapeutic approach.[14] Through this inhibition, PP2A-B55 activity could be amplified, leading to cell cycle arrest and subsequent apoptosis.

In this study, while much attention is given to PP2A-B55's central role in APC/C inactivation, other phosphatases may subtly yet significantly influence both mitotic progression and APC/C activity control. An intriguing area of interest, though not the focus of our current study, is the phosphatases responsible for Cdc20 dephosphorylation, which remain remarkably active even during mitosis (Figures 1D and 1F). To bind to the APC/C, Cdc20 needs to be dephosphorylated.[18,19] Although the specifics of Cdc20 dephosphorylation remain elusive, it is known that okadaic acid-sensitive phosphatases play a significant role[19] (Figure 1D). Apart from the reported roles of PP1[20,21] and PP2A,[19,22,23] other phosphatases, such as PP4, PP5, or PP6, might also contribute to Cdc20 dephosphorylation during

(E) Model overview: CDK1-PP2A-B55 interplay and its role in cell cycle oscillation through Apc1-loop^{300}. During interphase, inactive CDK1 allows PP2A-B55 to dephosphorylate Apc1-300L, preventing Cdc20 binding. Entering mitosis, activated CDK1 phosphorylates Apc1-300L and subsequently displaces of Apc1-300L, enabling the APC/C-Cdc20 complex formation and Cyclin B destruction. CDK1 also inhibits PP2A-B55 through the Gwl-Ensa/Arpp19 pathway, preserving this active state. Cdc20's interaction with the APC/C is dynamic. If PP2A-B55 activates prematurely (e.g., GwlΔ scenario), then it disrupts Cdc20's association, even if CDK is active. This effect can be counteracted by pEnsa (as indicated by GwlΔ+pEnsa), pinpointing PP2A-B55 as the principal regulator of Apc1-300L and Cdc20 dynamics. The APC/C functions as a pivotal substrate, with its activities fine-tuned by CDK and PP2A-B55, ensuring cell cycle oscillation.

mitosis. Furthermore, the involvement of PP1 in dephosphorylating Gwl and enhancing PP2A-B55 auto-activation has been reported.[30,31] Additionally, recent findings suggest that, once Cdc20 is associated with the APC/C, it becomes resistant to CDK1-mediated phosphorylation.[37] Despite these advances, unraveling the complex interplay of kinases and phosphatases during the cell cycle is essential for a comprehensive understanding of mitotic regulation.

A recent study by Mizrak and Morgan proposed that the interactions of Cdc20 and Cdh1 with APC/C in budding yeast lysates are influenced by polyanions.[38] Our experiments in *Xenopus* egg extracts seem to align with this proposal. We found that the dissociation of Cdc20 and Cdh1 from APC/C is a dynamic process. Interestingly, this dissociation remains unaffected by cell cycle stages but appears to be influenced by specific components within the extracts, akin to the role of polyanions observed in yeast. However, phospho-regulation seems to be the primary driver of APC/C-Cdc20 dynamics. This regulation is likely achieved through the differential kinetics of PP2A-B55 with phospho-threonine compared to phospho-serine residues.[23,35,36] This mechanism is particularly crucial during cell cycle stage transitions, such as the metaphase/anaphase transition, when CDK kinase activity starts to decline and opposing phosphatases begin to activate. In line with the previously established mathematical model,[39] we detected the highest APC/C-Cdc20 complex formation under conditions that experimentally mimic this transition (Figure 3E). We speculate that, at this stage, more dephosphorylated Cdc20 becomes available in the cytoplasmic pool, even though the Apc1-300L "gate" is on the verge of closing. As time progresses, both Cdc20 and Apc1-300L become fully dephosphorylated, leading to the closure of the gate and preventing further Cdc20 loading. This transition marks the switch from Cdc20 to Cdh1, another co-activator in the G1 phase, which then takes over the binding and activation of APC/C throughout the G1 phase.

In conclusion, our research has spotlighted Apc1-300L as a key substrate for CDK1 and PP2A-B55, orchestrating the rhythmic progression of the cell cycle. Through our detailed molecular analysis of Apc1-300L, we provide a foundational perspective, setting the stage for future studies in mitotic regulation.

Limitations of the study

While we have identified Apc1-300L as a key regulatory point, the APC/C complex features many other phosphorylation sites whose regulatory mechanisms await further exploration. Additionally, the delayed dephosphorylation of APC/C observed even with PP1 and PP2A-B55 inhibitors suggests a complex regulatory network involving other phosphatases, a topic that warrants deeper investigation. Conducted using cell-free *Xenopus* egg extracts, our research sets the stage for future *in vivo* studies to fully elucidate the intricate mechanisms governing APC/C activity, thereby enhancing our understanding of cell cycle regulation and its broader biological implications.

STAR★METHODS

Detailed methods are provided in the online version of this paper and include the following:

SUPPLEMENTAL INFORMATION

Supplemental information can be found online at https://doi.org/10.1016/j.celrep.2024.114155.

ACKNOWLEDGMENTS

We thank Drs. Julian Gannon, Helene Labit, Mathieu Bollen, Jakob Nilsson, and Thomas Mayer for providing reagents and information; the staff at the UCL Biological Services Unit for taking care of the *Xenopus* colony at UCL; and members of the Yamano laboratory for helpful discussions and critical reading of the manuscript. This work was supported by the Biotechnology and Biological Sciences Research Council (BB/N008383/1) and the Wellcome Trust (205150/Z/16/Z). Work in J.R.'s lab was supported by core funding from the Wellcome Trust (203149).

AUTHOR CONTRIBUTIONS

Conceptualization, K.H.C. and H.Y.; methodology, K.H.C., H.T., J.R., and H.Y.; investigation, K.H.C., H.T., K.F., S.D., J.Z., and H.Y.; writing – original draft, K.H.C. and H.Y.; writing – review & editing, all authors; funding acquisition, J.R and H.Y.; supervision, H.Y.

DECLARATION OF INTERESTS

The authors declare no competing interests.

Received: October 16, 2023
Revised: March 12, 2024
Accepted: April 10, 2024

REFERENCES

1. Mochida, S., and Hunt, T. (2012). Protein phosphatases and their regulation in the control of mitosis. EMBO Rep. *13*, 197–203.
2. Morgan, D.O. (2007). The Cell Cycle: Principles of Control (New Science Press).
3. Wurzenberger, C., and Gerlich, D.W. (2011). Phosphatases: providing safe passage through mitotic exit. Nat. Rev. Mol. Cell Biol. *12*, 469–482. https://doi.org/10.1038/nrm3149.
4. Watson, E.R., Brown, N.G., Peters, J.M., Stark, H., and Schulman, B.A. (2019). Posing the APC/C E3 Ubiquitin Ligase to Orchestrate Cell Division. Trends Cell Biol. *29*, 117–134. https://doi.org/10.1016/j.tcb.2018.09.007.

5. Barford, D. (2020). Structural interconversions of the anaphase-promoting complex/cyclosome (APC/C) regulate cell cycle transitions. Curr. Opin. Struct. Biol. *61*, 86–97. https://doi.org/10.1016/j.sbi.2019.11.010.

6. Primorac, I., and Musacchio, A. (2013). Panta rhei: The APC/C at steady state. J. Cell Biol. *201*, 177–189.

7. Pines, J. (2011). Cubism and the cell cycle: the many faces of the APC/C. Nat. Rev. Mol. Cell Biol. *12*, 427–438. https://doi.org/10.1038/nrm3132.

8. Yamano, H. (2019). APC/C: current understanding and future perspectives. F1000Res. *8*, F1000 Faculty Rev-725. https://doi.org/10.12688/f1000research.18582.1.

9. Ubersax, J.A., Woodbury, E.L., Quang, P.N., Paraz, M., Blethrow, J.D., Shah, K., Shokat, K.M., and Morgan, D.O. (2003). Targets of the cyclin-dependent kinase Cdk1. Nature *425*, 859–864.

10. Dephoure, N., Zhou, C., Villén, J., Beausoleil, S.A., Bakalarski, C.E., Elledge, S.J., and Gygi, S.P. (2008). A quantitative atlas of mitotic phosphorylation. Proc. Natl. Acad. Sci. USA *105*, 10762–10767. https://doi.org/10.1073/pnas.0805139105.

11. Mochida, S., Ikeo, S., Gannon, J., and Hunt, T. (2009). Regulated activity of PP2A-B55 delta is crucial for controlling entry into and exit from mitosis in Xenopus egg extracts. EMBO J. *28*, 2777–2785.

12. Wu, J.Q., Guo, J.Y., Tang, W., Yang, C.S., Freel, C.D., Chen, C., Nairn, A.C., and Kornbluth, S. (2009). PP1-mediated dephosphorylation of phosphoproteins at mitotic exit is controlled by inhibitor-1 and PP1 phosphorylation. Nat. Cell Biol. *11*, 644–651.

13. Schmitz, M.H.A., Held, M., Janssens, V., Hutchins, J.R.A., Hudecz, O., Ivanova, E., Goris, J., Trinkle-Mulcahy, L., Lamond, A.I., Poser, I., et al. (2010). Live-cell imaging RNAi screen identifies PP2A-B55alpha and importin-beta1 as key mitotic exit regulators in human cells. Nat. Cell Biol. *12*, 886–893. https://doi.org/10.1038/ncb2092.

14. Manchado, E., Guillamot, M., de Cárcer, G., Eguren, M., Trickey, M., García-Higuera, I., Moreno, S., Yamano, H., Cañamero, M., and Malumbres, M. (2010). Targeting mitotic exit leads to tumor regression in vivo: Modulation by Cdk1, Mastl, and the PP2A/B55alpha,delta phosphatase. Cancer Cell *18*, 641–654.

15. Fujimitsu, K., Grimaldi, M., and Yamano, H. (2016). Cyclin-dependent kinase 1-dependent activation of APC/C ubiquitin ligase. Science *352*, 1121–1124. https://doi.org/10.1126/science.aad3925.

16. Zhang, S., Chang, L., Alfieri, C., Zhang, Z., Yang, J., Maslen, S., Skehel, M., and Barford, D. (2016). Molecular mechanism of APC/C activation by mitotic phosphorylation. Nature *533*, 260–264. https://doi.org/10.1038/nature17973.

17. Qiao, R., Weissmann, F., Yamaguchi, M., Brown, N.G., VanderLinden, R., Imre, R., Jarvis, M.A., Brunner, M.R., Davidson, I.F., Litos, G., et al. (2016). Mechanism of APC/CCDC20 activation by mitotic phosphorylation. Proc. Natl. Acad. Sci. USA *113*, E2570–E2578. https://doi.org/10.1073/pnas.1604929113.

18. Yudkovsky, Y., Shteinberg, M., Listovsky, T., Brandeis, M., and Hershko, A. (2000). Phosphorylation of Cdc20/fizzy negatively regulates the mammalian cyclosome/APC in the mitotic checkpoint. Biochem. Biophys. Res. Commun. *271*, 299–304.

19. Labit, H., Fujimitsu, K., Bayin, N.S., Takaki, T., Gannon, J., and Yamano, H. (2012). Dephosphorylation of Cdc20 is required for its C-box-dependent activation of the APC/C. EMBO J. *31*, 3351–3362.

20. Kim, T., Lara-Gonzalez, P., Prevo, B., Meitinger, F., Cheerambathur, D.K., Oegema, K., and Desai, A. (2017). Kinetochores accelerate or delay APC/C activation by directing Cdc20 to opposing fates. Genes Dev. *31*, 1089–1094. https://doi.org/10.1101/gad.302067.117.

21. Bancroft, J., Holder, J., Geraghty, Z., Alfonso-Pérez, T., Murphy, D., Barr, F.A., and Gruneberg, U. (2020). PP1 promotes cyclin B destruction and the metaphase-anaphase transition by dephosphorylating CDC20. Mol. Biol. Cell *31*, 2315–2330. https://doi.org/10.1091/mbc.E20-04-0252.

22. Fujimitsu, K., and Yamano, H. (2020). PP2A-B56 binds to Apc1 and promotes Cdc20 association with the APC/C ubiquitin ligase in mitosis. EMBO Rep. *21*, e48503. https://doi.org/10.15252/embr.201948503.

23. Hein, J.B., Hertz, E.P.T., Garvanska, D.H., Kruse, T., and Nilsson, J. (2017). Distinct kinetics of serine and threonine dephosphorylation are essential for mitosis. Nat. Cell Biol. *19*, 1433–1440. https://doi.org/10.1038/ncb3634.

24. Yu, J., Zhao, Y., Li, Z., Galas, S., and Goldberg, M.L. (2006). Greatwall kinase participates in the Cdc2 autoregulatory loop in Xenopus egg extracts. Mol. Cell *22*, 83–91. https://doi.org/10.1016/j.molcel.2006.02.022.

25. Mochida, S., Maslen, S.L., Skehel, M., and Hunt, T. (2010). Greatwall phosphorylates an inhibitor of protein phosphatase 2A that is essential for mitosis. Science *330*, 1670–1673.

26. Gharbi-Ayachi, A., Labbé, J.C., Burgess, A., Vigneron, S., Strub, J.M., Brioudes, E., Van-Dorsselaer, A., Castro, A., and Lorca, T. (2010). The substrate of Greatwall kinase, Arpp19, controls mitosis by inhibiting protein phosphatase 2A. Science *330*, 1673–1677. https://doi.org/10.1126/science.1197048.

27. Holder, J., Poser, E., and Barr, F.A. (2019). Getting out of mitosis: spatial and temporal control of mitotic exit and cytokinesis by PP1 and PP2A. FEBS Lett. *593*, 2908–2924. https://doi.org/10.1002/1873-3468.13595.

28. Castilho, P.V., Williams, B.C., Mochida, S., Zhao, Y., and Goldberg, M.L. (2009). The M phase kinase Greatwall (Gwl) promotes inactivation of PP2A/B55delta, a phosphatase directed against CDK phosphosites. Mol. Biol. Cell *20*, 4777–4789. https://doi.org/10.1091/mbc.e09-07-0643.

29. Vigneron, S., Brioudes, E., Burgess, A., Labbé, J.C., Lorca, T., and Castro, A. (2009). Greatwall maintains mitosis through regulation of PP2A. EMBO J. *28*, 2786–2793.

30. Heim, A., Konietzny, A., and Mayer, T.U. (2015). Protein phosphatase 1 is essential for Greatwall inactivation at mitotic exit. EMBO Rep. *16*, 1501–1510. https://doi.org/10.15252/embr.201540876.

31. Ma, S., Vigneron, S., Robert, P., Strub, J.M., Cianferani, S., Castro, A., and Lorca, T. (2016). Greatwall dephosphorylation and inactivation upon mitotic exit is triggered by PP1. J. Cell Sci. *129*, 1329–1339. https://doi.org/10.1242/jcs.178855.

32. Schmidt, A., Duncan, P.I., Rauh, N.R., Sauer, G., Fry, A.M., Nigg, E.A., and Mayer, T.U. (2005). Xenopus polo-like kinase Plx1 regulates XErp1, a novel inhibitor of APC/C activity. Genes Dev. *19*, 502–513.

33. Tung, J.J., Hansen, D.V., Ban, K.H., Loktev, A.V., Summers, M.K., Adler, J.R., 3rd, and Jackson, P.K. (2005). A role for the anaphase-promoting complex inhibitor Emi2/XErp1, a homolog of early mitotic inhibitor 1, in cytostatic factor arrest of Xenopus eggs. Proc. Natl. Acad. Sci. USA *102*, 4318–4323.

34. Tischer, T., Hörmanseder, E., and Mayer, T.U. (2012). The APC/C inhibitor XErp1/Emi2 is essential for Xenopus early embryonic divisions. Science *338*, 520–524. https://doi.org/10.1126/science.1228394.

35. Cundell, M.J., Hutter, L.H., Nunes Bastos, R., Poser, E., Holder, J., Mohammed, S., Novak, B., and Barr, F.A. (2016). A PP2A-B55 recognition signal controls substrate dephosphorylation kinetics during mitotic exit. J. Cell Biol. *214*, 539–554. https://doi.org/10.1083/jcb.201606033.

36. Godfrey, M., Touati, S.A., Kataria, M., Jones, A., Snijders, A.P., and Uhlmann, F. (2017). PP2A(Cdc55) Phosphatase Imposes Ordered Cell-Cycle Phosphorylation by Opposing Threonine Phosphorylation. Mol. Cell *65*, 393–402.e3. https://doi.org/10.1016/j.molcel.2016.12.018.

37. Shevah-Sitry, D., Miniowitz-Shemtov, S., Teichner, A., Kaisari, S., and Hershko, A. (2022). Role of phosphorylation of Cdc20 in the regulation of the action of APC/C in mitosis. Proc. Natl. Acad. Sci. USA *119*, e2210367119. https://doi.org/10.1073/pnas.2210367119.

38. Mizrak, A., and Morgan, D.O. (2019). Polyanions provide selective control of APC/C interactions with the activator subunit. Nat. Commun. *10*, 5807. https://doi.org/10.1038/s41467-019-13864-1.

39. Ciliberto, A., Lukács, A., Tóth, A., Tyson, J.J., and Novák, B. (2005). Rewiring the exit from mitosis. Cell Cycle *4*, 1107–1112.

40. Zhang, Z., Yang, J., and Barford, D. (2016). Recombinant expression and reconstitution of multiprotein complexes by the USER cloning method in the insect cell-baculovirus expression system. Methods *95*, 13–25. https://doi.org/10.1016/j.ymeth.2015.10.003.

41. Fujimitsu, K., and Yamano, H. (2021). Dynamic regulation of mitotic ubiquitin ligase APC/C by coordinated Plx1 kinase and PP2A phosphatase action on a flexible Apc1 loop. EMBO J. *40*, e107516. https://doi.org/10.15252/embj.2020107516.

42. Mendes, M.L., Fischer, L., Chen, Z.A., Barbon, M., O'Reilly, F.J., Giese, S.H., Bohlke-Schneider, M., Belsom, A., Dau, T., Combe, C.W., et al. (2019). An integrated workflow for crosslinking mass spectrometry. Mol. Syst. Biol. *15*, e8994. https://doi.org/10.15252/msb.20198994.

43. Murray, A.W. (1991). Cell cycle extracts. Methods Cell Biol. *36*, 581–605.

44. Yamano, H., Trickey, M., Grimaldi, M., and Kimata, Y. (2009). In vitro assays for the anaphase-promoting complex/cyclosome (APC/C) in Xenopus egg extracts. Methods Mol. Biol. *545*, 287–300.

45. Beullens, M., Vulsteke, V., Van Eynde, A., Jagiello, I., Stalmans, W., and Bollen, M. (2000). The C-terminus of NIPP1 (nuclear inhibitor of protein phosphatase-1) contains a novel binding site for protein phosphatase-1 that is controlled by tyrosine phosphorylation and RNA binding. Biochem. J. *352*, 651–658.

46. Kruse, T., Gnosa, S.P., Nasa, I., Garvanska, D.H., Hein, J.B., Nguyen, H., Samsøe-Petersen, J., Lopez-Mendez, B., Hertz, E.P.T., Schwarz, J., et al. (2020). Mechanisms of site-specific dephosphorylation and kinase opposition imposed by PP2A regulatory subunits. EMBO J. *39*, e103695. https://doi.org/10.15252/embj.2019103695.

47. Maiolica, A., Cittaro, D., Borsotti, D., Sennels, L., Ciferri, C., Tarricone, C., Musacchio, A., and Rappsilber, J. (2007). Structural analysis of multiprotein complexes by cross-linking, mass spectrometry, and database searching. Mol. Cell. Proteomics *6*, 2200–2211. https://doi.org/10.1074/mcp.M700274-MCP200.

48. Rappsilber, J., Ishihama, Y., and Mann, M. (2003). Stop and go extraction tips for matrix-assisted laser desorption/ionization, nanoelectrospray, and LC/MS sample pretreatment in proteomics. Anal. Chem. *75*, 663–670. https://doi.org/10.1021/ac026117i.

49. Kessner, D., Chambers, M., Burke, R., Agus, D., and Mallick, P. (2008). ProteoWizard: open source software for rapid proteomics tools development. Bioinformatics *24*, 2534–2536. https://doi.org/10.1093/bioinformatics/btn323.

50. Lenz, S., Giese, S.H., Fischer, L., and Rappsilber, J. (2018). In-Search Assignment of Monoisotopic Peaks Improves the Identification of Cross-Linked Peptides. J. Proteome Res. *17*, 3923–3931. https://doi.org/10.1021/acs.jproteome.8b00600.

51. Perez-Riverol, Y., Bai, J., Bandla, C., García-Seisdedos, D., Hewapathirana, S., Kamatchinathan, S., Kundu, D.J., Prakash, A., Frericks-Zipper, A., Eisenacher, M., et al. (2022). The PRIDE database resources in 2022: a hub for mass spectrometry-based proteomics evidences. Nucleic Acids Res. *50*, D543–D552. https://doi.org/10.1093/nar/gkab1038.

STAR★METHODS

KEY RESOURCES TABLE

REAGENT or RESOURCE	SOURCE	IDENTIFIER
Antibodies		
Rabbit polyclonal anti-Apc1 (pS314/pS318)	Lab stock	#25312 via BioGenes
Rabbit polyclonal anti-Apc1 (pS358)	This paper	#27644 via BioGenes
Rabbit polyclonal anti-Apc1 (pT378/pS380)	This paper	#25316 via BioGenes
Rabbit polyclonal anti-Apc1	Lab stock	#4853 via BioGenes
Rabbit polyclonal anti-Apc2	Lab stock	#7576 and #7577 via BioGenes
Mouse monoclonal anti-Cdc27/Apc3	BD Biosciences	610455; RRID:AB_397828
Mouse monoclonal anti-Apc3 (AF3.1)	Gift from J. Gannon	N/A
Rabbit polyclonal anti-Apc5	Lab stock	#3445 via BioGenes
Rabbit polyclonal anti-Apc6	Lab stock	#3447 via BioGenes
Rabbit polyclonal anti-Gwl	Lab stock	#7387 via BioGenes
Rabbit polyclonal anti-XErp1	Lab stock	#8344 via BioGenes
Mouse monoclonal anti-FLAG (M2)	Sigma-Aldrich	F1804; RRID:AB_262044
Mouse monoclonal anti-Cyclin B (X121)	Gift from J. Gannon	N/A
Mouse monoclonal anti-Cdc20 (BA8.1)	Gift from J. Gannon	N/A
Mouse monoclonal anti-6xHis	Clontech	Cat#631212; RRID:AB_2721905
Mouse monoclonal anti-phosphorylated Plx1 (AZ44)	Gift from J. Gannon	N/A
Goat anti-mouse immunoglobulins, HRP-conjugated	Dako	Cat#P0447; RRID:AB_2617137
Swine anti-rabbit immunoglobulins, HRP-conjugated	Dako	Cat#P0217; RRID:AB_2728719
IRDye 680RD goat anti-mouse immunoglobulins	LI-COR Biosciences	Cat#926–68070; RRID:AB_2651128
IRDye 800CW goat anti-rabbit immunoglobulins	LI-COR Biosciences	Cat#926–32211; RRID:AB_2651127
Bacterial and virus strains		
Escherichia coli DH5α	Lab stock	N/A
Escherichia coli BL21-CodonPlus (DE3)-RIL	Agilent	Cat#230245
Multibac baculovirus/insect cell system	Zhang Z. et al.[40] and Fujimitsu K. et al.[15]	N/A
Chemicals, peptides, and recombinant proteins		
ATP	Sigma-Aldrich	Cat#10519979001
ATPγS	Calbiochem	Cat#119120
[γ-P32]ATP, 6000 Ci/mmol, 10 mCi/mL	Hartmann Analytic	SRP-501
[S35]Met-label, 1000 Ci/mmol, 10 mCi/mL	Hartmann Analytic	SCIS-103
Cycloheximide	Sigma-Aldrich	Cat#C7698
Okadaic acid	Sigma-Aldrich	Cat#O4511
MG132 proteasome inhibitor	Calbiochem	Cat#474790
Desthiobiotin	Sigma-Aldrich	Cat#D1411
Lysozyme	Sigma-Aldrich	Cat#L6876
Benzonase	MILLIPORE	Cat#70746
Methylated ubiquitin	Sigma-Aldrich	Cat#662065
3FLAG-Ub-Cyclin B-N70-KA (Ub-K0-Cyclin B)	Fujimitsu K. and Yamano H.[41]	N/A
GST-Cyclin BΔ167	Gift from J. Gannon	pGEX Hs cyclin BΔ167
CDK2-Cyclin A complex	Gift from J. Gannon	N/A
GST-PreScission protease	Lab stock	N/A
10His-ENSA	Lab stock	Plasmid stock #1523

(*Continued on next page*)

Continued

REAGENT or RESOURCE	SOURCE	IDENTIFIER
10His-NIPP1 (amino acids 143–224)	This paper	N/A
MBP-4LxxIxE-6His	This paper	N/A
MBP-4AxxAxA-6His	This paper	N/A
3FLAG-Apc1-300L-6His (WT and mutants)	This paper	N/A
Recombinant APC/C complexes (WT and mutant)	This paper	N/A
PP2A-B55 complex	This paper	N/A
Critical commercial assays		
USER Cloning kit	New England Biolabs	Cat#M5505
TNT T7 Quick Coupled Transcription/Translation System	Promega	Cat#L1170
Quick CIP	New England Biolabs	Cat#M0525
Pierce ECL Western Blotting Substrate	Thermo Fisher Scientific	Cat#32106
Deposited data		
Crosslinking identification	PRIDE	PXD050097
Experimental models: Cell lines		
Spodoptera frugiperda (Sf9) insect cells	Gibco	B82501
Trichoplusia ni (High Five) insect cells	Invitrogen	B85502
Experimental models: Organisms/strains		
Xenopus laevis females	NASCO	N/A
Oligonucleotides		
Oligonucleotide PCR primers (sequences available on request)	Integrated DNA Technologies	N/A
Recombinant DNA		
gBlock DNA (4LxxIxE motifs)	This study; Integrated DNA Technologies	N/A
gBlock DNA (4AxxAxA motifs)	This study; Integrated DNA Technologies	N/A
pET-3FLAG-Apc1-300L-6His (WT)	Lab stock[22]	N/A
pET-3FLAG-Apc1-300L-6His (7T)	Lab stock[22]	N/A
pET-3FLAG-Apc1-300L-6His (7A)	Lab stock	Plasmid stock #2195
pET-3FLAG-Apc1-300L-6His (S314-6A)	This paper	Plasmid stock #1913
pET-3FLAG-Apc1-300L-6His (S318-6A)	This paper	Plasmid stock #1914
pET-3FLAG-Apc1-300L-6His (S335-6A)	This paper	Plasmid stock #1915
pET-3FLAG-Apc1-300L-6His (S344-6A)	This paper	Plasmid stock #1916
pET-3FLAG-Apc1-300L-6His (S358-6A)	This paper	Plasmid stock #1917
pET-3FLAG-Apc1-300L-6His (S380-6A)	This paper	Plasmid stock #1918
pET-3FLAG-Apc1-300L-6His (S389-6A)	This paper	Plasmid stock #1919
pET16b-4LxxIxE-6His	This paper	Plasmid stock #2506
pET16b-4AxxAxA-6His	This paper	Plasmid stock #2507
pMal-Cdc20-N159-4A (T79)-6His	Lab stock	Plasmid stock #1552
pHY22-3FLAG-Cdc20-5A	This paper	Plasmid stock #1908
pHY22-Cdc20-5A	Lab stock	Plasmid stock #1017
pHY22-3FLAG-Cdh1-4A	This study	Plasmid stock #1910
pHY22-Cdc13 (Cyclin B)	Lab stock	Plasmid stock #372
pHY22-Cdc13Δ67 (Cyclin BΔ67)	Lab stock	Plasmid stock #373
pHY22-NEK2A (Nek2A)	Lab stock	Plasmid stock #647
pFUBB-Apc2/Apc11-Apc1/Apc10 (WT and mutant)	Lab stock	N/A
pFUBB-Apc3/Apc8/Apc7-Apc5/Apc4/Apc6-StrepII	Lab stock	N/A
pUUBB-Apc13-Apc12/Apc15/Apc16	Lab stock	N/A

(*Continued on next page*)

Continued

REAGENT or RESOURCE	SOURCE	IDENTIFIER
pFUBB-PP2A-Cβ-His-B55δ	This paper	N/A
pUUBB-GST-PP2A-Aα	Lab stock, Fujimitsu K.and Yamano H.[22]	N/A
Software and algorithms		
ImageJ	National Institutes of Health	RRID:SCR_003070
Image Studio Lite	LI-COR	RRID:SCR_013715
Adobe Illustrator	Adobe	RRID:SCR_010279
SnapGene	SnapGene	RRID:SCR_015052
ClustalW	GenomeNet, Kyoto University Bioinformatics Center	RRID:SCR_017277
Xi software (version 1.7.6.4)	Juri Rappsilber Lab[42]	https://www.rappsilberlab.org/software/
Other		
Dynabeads Protein A	Invitrogen	Cat#10001D
Pierce Protein A/G Magnetic Beads	Thermo Fisher Scientific	Cat#88803
HisPur Ni-NTA Magnetic Beads	Thermo Fisher Scientific	Cat#88831
Ni-NTA Agarose	Qiagen	Cat#30210
Anti-FLAG M2 Affinity Gel	Sigma-Aldrich	Cat#A2220
Glutathione Sepharose 4B	Cytiva	Cat#17075601
Strep-Tactin SuperFlow Plus	Qiagen	Cat#30004

RESOURCE AVAILABILITY

Lead contact

Further information and requests for resources and reagents should be directed to and will be fulfilled by the lead contact, Hiroyuki Yamano (h.yamano@ucl.ac.uk).

Materials availability

All unique reagents generated in this study are available from the lead contact upon request.

Data and code availability

- All data reported in this paper will be shared by the lead contact upon request. The CLMS data have been deposited to the ProteomeXchange Consortium via the PRIDE partner repository with the dataset identifier ProteomeXchange: PXD050097 and PRoteomics IDEntifications (PRIDE) Database: PXD050097.
- This paper does not report original code.
- Any additional information required to analyze the data reported in this paper is available from the lead contact upon request.

EXPERIMENTAL MODEL AND STUDY PARTICIPANT DETAILS

Xenopus laevis

The experimental model utilizes extracts prepared from eggs obtained through the superovulation of adult female *Xenopus laevis* (NASCO). This procedure has received approval from the University College London (UCL) Animal Welfare and Ethical Review Body (AWERB), ensuring compliance with all pertinent regulatory standards and guidelines established by the Home Office. Named Animal Care and Welfare Officers (NACWOs) alongside UCL Biological Services Unit staff are responsible for the animals' daily care, welfare, and husbandry. Additionally, Named Veterinary Surgeons (NVSs) oversee the health, welfare, and medical treatment of the animals, ensuring our research adheres to the highest ethical and care standards.

METHOD DETAILS

Preparation of *Xenopus* egg extracts

Cytostatic factor-arrested *Xenopus laevis* egg extract, also known as CSF extract, was prepared as the previously described method.[43,44] To prepare interphase extract, 10 μg/mL cycloheximide and 0.4 mM $CaCl_2$ were supplemented to CSF extract at 23°C, and the extract was incubated for 1.5 h for the progression from meiotic metaphase II to interphase. Anaphase extract was

prepared by incubating interphase extract at 23°C for 60 min in the presence of nondegradable GST-fused human Cyclin B lacking the N-terminal 167 amino acids (Cyclin BΔ167). Cdc20-depleted extracts were obtained following the previously described immunodepletion method,[44] but APC/C-depleted extracts were prepared by sequential depletion of Apc2 and Apc3 using their respective antibody-conjugated Dynabeads Protein A (Invitrogen). For Gwl or XErp1 depletion, only one round of depletion was performed using their respective antibody-bound Pierce Protein A/G magnetic beads (Thermo Fisher Scientific).

Antibodies

Antibodies used in immunodepletion are as follows: Apc2 (RbAb 7576), Apc3 (MAb AF3.1), Gwl (RbAb 7387), Cdc20 (RbAb B60), and XErp1 (RbAb 8344). For immunoblotting, antibodies and their dilution ratio are as follows: Apc1 (RbAb 4853; 1:100), Apc2 (RbAb 7577; 1:1000), Apc3/Cdc27 (BD Transduction Laboratories; 1:200), Apc5 (RbAb 3445; 1:500), Apc6 (RbAb 3447; 1:500), Gwl (RbAb 7387; 1:400), FLAG M2 (Sigma; 1:1000), Cyclin B (MAb X121; 1:2), XErp1 (RbAb 8344; 1:50), Cdc20 (MAb BA8.1; 1:50), 6xHis (Clontech; 1:500), pPlx1 (MAb AZ44; 1:1000), goat anti-mouse immunoglobulins HRP-conjugated (Dako; 1:5000), swine anti-rabbit immunoglobulins HRP-conjugated (Dako; 1:5000), IRDye 680RD goat anti-mouse immunoglobulins (LI-COR Biosciences; 1:1000), and IRDye 800CW goat anti-rabbit immunoglobulins (LI-COR Biosciences; 1:5000). Apc1 phospho-specific antibodies: pS314/pS318 (RbAb 25312; 1:200), pS358 (RbAb 27644; 1:100), pT378/pS380 (RbAb 25316; 1:400) were raised in rabbits against LPH (the horseshoe crab Limulus polyphemus hemocyanin) conjugated phosphopeptides CVSKGEpSPTApSPFQN, CLSRSHpSPALGV and CFSSNpTPpSPKR, respectively (BioGenes, Germany). Antibodies were affinity purified using a phosphopeptide column prepared with SulfoLink Kit (Pierce). After elution with ImmunoPure Gentle Ag/Ab Elution Buffer (Pierce), antibodies were dialyzed against TBS and non-phosphospecific antibody was affinity depleted by passing through a column cross-linked with non-phosphopeptides CVSKGESPTASPFQN, CLSRSHSPALGV and CFSSNTPSPKR. The eluted phospho-specific antibodies were then enriched by dialysis against TBS containing 50% glycerol.

Plasmid/bacmid construction and mutagenesis

Cloning of the Apc1-300L fragment (amino acids 294–399 of *Xenopus* Apc1), its 7A and 7T derivatives tagged with 3FLAGs and 6His have been reported previously.[15] To generate a series of plasmids containing Apc1-300L with single site for CDK phosphorylation, PCR-based site-directed mutagenesis was performed for single serine substitution on the 7A derivative plasmid. Plasmid for expression and purification of 10His-tagged NIPP1 fragment (amino acids 143–224) was a gift from Dr. Bollen.[45] The gBlock gene fragment containing four LxxIxE motifs[46] (LPRSSTLPTIHEEEELSLC) ordered from Integrated DNA Technologies was cloned into the pET16b vector to generate the MBP-4LxxIxE-6His construct for the expression and purification of PP2A-B56 inhibitor (B56i). Full length Cdc20-5A and the MBP-Cdc20-N159-4A (hereafter Cdc20-T79) constructs have been reported previously.[19] Cdc20-5A was further subcloned into a pHY22 plasmid containing 3FLAGs to generate the FLAG-Cdc20-5A construct. Bacmid construction for the reconstitution of wild type and Apc1-300LΔ APC/C complexes have been reported previously.[15,22] For the reconstitution of PP2A-B55 holoenzyme complex, three PP2A subunit genes (Aα, B55δ and Cβ) were amplified by PCR and cloned into pOENmyc vector with polH promoter and SV40 terminator for Cβ, and p10 promoter and HSVtk terminator for Aα and B55δ, respectively. PreScission protease-cleavable GST-tag and His-tag was fused to Aα and B55δ, respectively, at the N terminus. These genes were further cloned into MultiBac vectors creating one pF1 vector-derivative pFUBB carrying Cβ at MUM1 site and His-B55δ at MUM2 site. A pU1 vector-derivative pUUBB carrying Aα at MUM2 site was also created. After sequence confirmation, the baculovirus was generated.

Recombinant proteins

All His-fused recombinant proteins were expressed in BL21-CodonPlus (DE3) bacteria at 18°C for 16–18 h in the presence of 0.1 mM IPTG. Bacterial cells were lysed by 2 mg/mL lysozyme and sonicated in IMAC-5 buffer (20 mM Tris-HCL pH 8, 500 mM NaCl, 5 mM imidazole) supplemented with 5 mM EGTA, 1 mM PMSF, 10 μg/mL leupeptin, 10 μg/mL pepstatin A and 10 μg/mL chymostatin, and 0.5% NP-40. Proteins were purified from clarified lysate on Ni-NTA agarose beads (Qiagen), eluted with elution buffer (20 mM Tris-HCl pH 8, 150 mM NaCl, 0.4 M imidazole), and dialyzed with dialysis buffer (50 mM HEPES pH 7.9, 125 mM NaCl, 10% glycerol). Expression of the FLAG-Cdc20-5A was carried out using the TNT Quick Coupled Transcription/Translation System (Promega). Thio-phosphorylation of Ensa was carried out by incubating purified Ensa in kinase buffer (20 mM Tris-HCl pH 7.5, 20 mM KCl, 60 mM NaCl, 1 mM EGTA, 40 mM β-glycerophosphate, 10 mM $MgCl_2$, 2 mM DTT, 4 mM $MnCl_2$, and 60 nM okadaic acid) containing immunoprecipitated Gwl from CSF extract and 1 mM ATPγS at 23°C. After separation from the immunoprecipitated Gwl, supernatant was dialyzed with dialysis buffer. For the expression and purification of rAPC/C complexes, baculoviruses were generated from Sf9 insect cells using the constructed bacmids. The rAPC/C complexes were expressed using High Five insect cells (Invitrogen), and purification of rAPC/C was carried out essentially as described previously.[15] All purification steps were performed at 4°C. The same method was used for the expression of PP2A-B55 holoenzyme complex, except that the baculovirus was used at MOI of 2 for expression. Purification of PP2A-B55 holoenzyme was performed by lysing the cells in PP2A lysis buffer [50 mM Tris-HCl pH 7.5, 150 mM NaCl, 0.5 mM DTT, 0.1% Tween 20, 1 mM EGTA, 5% glycerol, 10 μg/mL leupeptin, 10 μg/mL pepstatin A, 10 μg/mL chymostatin, and 30 units/mL benzonase (Novagen)] through sonication, followed by centrifugation at 18,800×*g* for 20 min. The resultant supernatant was centrifuged again for 20 min, and the cleared lysate was incubated with Glutathione Sepharose 4B beads (GE Healthcare) for 1 h. The beads were washed twice with PP2A wash buffer 1 (50 mM Tris-HCl pH 7.5, 150 mM NaCl, 0.5 mM DTT, 0.1% Tween 20, 1 mM EGTA, and 1 mM EDTA) and once with PP2A wash buffer 2 (50 mM Tris-HCl pH 7.5, 150 mM

NaCl, 0.5 mM DTT, 1 mM EDTA, and 5% glycerol), and suspended into PP2A wash buffer 2 containing PreScission protease for 17 h incubation with gentle mixing. Supernatant was recovered and kept at −80°C.

Kinase and phosphatase assays

To validate phosphorylation of Apc1-300L, 140 ng of purified Apc1-300L or its derivative (7T or 7A) was incubated at 30°C for 1 h in 20 μL of kinase buffer (20 mM HEPES pH 7.8, 10 mM $MgCl_2$, 15 mM KCl, 1 mM EGTA, and 0.05% NP-40) in the presence of [γ-^{32}P]-ATP (Hartmann Analytic) and recombinant CDK-Cyclin A. Reaction was stopped with 20 mM of ATP and analyzed by SDS-PAGE and autoradiography. To prepare phosphorylated proteins, purified Apc1-300L (140 ng) and Cdc20-T79 (10 μg) were used in their corresponding phosphorylation assay. Reactions were incubated for 2 h and stopped with ATP prior to use in dephosphorylation assays or storage at −80°C. For the assay in Figure 1C, the ^{32}P-labelled Apc1-300L (3.5 ng), or Cdc20-T79 (250 ng) was added to CSF extract containing 150 μM MG132 at 23°C, in the presence of DMSO or 2 μM okadaic acid, to start the reactions. For Figures 1E and 1G, MG132 supplemented CSF extract was first treated with Gwl antibody-bound beads (Gwl-depletion) or empty beads mock depletion, and pEnsa (5 μM) or XB-CSF buffer was added before separating from beads. Cdc20-T79 (500 ng) was complemented to the recovered extracts at 23°C to start the reactions. For the assays using Apc1-300L as substrate, 3.9 ng of ^{32}P-Apc1-300L was added to the CSF extract containing MG132 in Figures 1E and 1G or the anaphase extracts supplemented with phosphatase inhibitors in Figure S2A, prior to the dephosphorylation reactions trigger by immunodepletion or addition of 0.35 μM p27, respectively. Samples taken at the indicated time points were mixed with SDS sample buffer, followed by analysis using SDS-PAGE and autoradiography. For the *in vitro* phosphatase assay in Figure 2D, purified Apc1-300L (375 ng) was phosphorylated with CDK-Cyclin A in the presence of 1 mM ATP in 10 μL kinase buffer as described above, and the reaction was stopped with 1 μM of ATP. Purified PP2A-B55 holoenzyme complex from insect cells was incubated with the HisPur Ni-NTA magnetic beads (Thermo Fisher Scientific) at 4°C for 20 min, and the recovered beads were washed twice with kinase buffer. The beads containing PP2A-B55 complex were then mixed with 10 μL of the prepared kinase reaction containing phosphorylated Apc1-300L at 23°C in the presence or absence of 10 μM pEnsa. Samples taken at the indicated time points were mixed with SDS sample buffer prior to analyzed by SDS-PAGE and immunoblotting using indicated antibodies.

Destruction and ubiquitylation assays

Destruction assays were performed essentially as described previously.[44] Substrates, including Nek2A, Cyclin B, and Cyclin BΔ67 (a variant lacking the D-box, thus rendering it a stable Cyclin B form), were labeled with [^{35}S]methionine (Hartmann Analytic) using the TNT Quick Coupled Transcription/Translation System (Promega). Destruction assays were then carried out using *Xenopus* egg cell-free extracts. Samples were taken at the indicated time points and analyzed by SDS-PAGE and autoradiography. For rAPC/C-mediated destruction assays, purified recombinant APC/Cs were first phosphorylated by incubating with the MG132 supplemented CSF extract lacking endogenous APC/C (APC/C-depleted) at 23°C for 1 h. Phosphorylated rAPC/Cs were recovered and added to the indicated APC/C-depleted anaphase extracts and samples were taken immediately to check the amount of rAPC/C. The extracts supplemented with rAPC/C were incubated at 23°C for 40 min, prior to addition of ^{35}S-labelled substrates. Samples taken at the indicated time points were mixed with SDS sample buffer, followed by analysis using SDS-PAGE and autoradiography. *In vitro* ubiquitylation assay was performed as described previously.[41] Endogenous APC/C complex was first immunoprecipitated from the indicated CSF and interphase extracts, using the Apc3 antibody immobilized Dynabeads as used in immunodepletion. The beads were washed twice with XB-CSF buffer[44] supplemented with extra 200 mM KCl and 0.01% NP-40, and once with Ub buffer (20 mM Tris-HCl pH 7.5, 100 mM KCl, 2.5 mM $MgCl_2$, and 0.3 mM DTT) containing 0.01% NP-40. The purified APC/C-Cdc20 complexes were then incubated in 20 μL of Ub buffer at 23°C in the presence of 2 mM ATP, 50 ng/μL E1, 6 ng/μL Ube2S, 750 ng/μL methylated ubiquitin (MeUb) and 5 ng/μL FLAG-ubiquitin-fused Cyclin B-N70 fragment (N-terminal 70 residues) with alanine substitution of all lysine residues, referred to as Ub-K0-Cyclin B, as a substrate. Samples taken at the indicated time points were mixed with SDS sample buffer prior to analyzed by SDS-PAGE and immunoblotting using indicated antibodies. Activity of APC/C can be determined by quantification of monoubiquitylated substrates as polyubiquitin chain formation is prevented by MeUb.

Binding assay and Cdc20 *de novo* loading assays

Immunoprecipitation of APC/C complex from *Xenopus* egg extracts was carried out using Dynabeads Protein A (Invitrogen) conjugated with Apc3 antibody AF3.1 (Apc3-beads). Conjugation procedure is same as described in immunodepletion.[44] Apc3-beads were incubated with the indicated extracts at 23°C for 10 min for the experiments in Figure 3E and 5 min for the experiments in Figure S3D. The resultant beads were washed twice with XB-CSF containing 300 mM KCl and 0.01% NP-40, split into two equal portions, and subjected to elution with SDS sample buffer and phosphatase treatment, respectively. Phosphatase treatment was performed using the Quick CIP (New England Biolabs), to facilitate the quantification of Cdc20 co-immunoprecipitated with APC/C. The same immunoprecipitation procedure was carried out in performing the *de novo* loading assays in Figure 4D and Figure S4G. For Figure 4D, the *in vitro* translated FLAG-Cdc20-5A was added to egg extract together with the Apc3-beads to evaluate the association of the FLAG-Cdc20-5A with APC/C during the process. For Figure S4G, purified rAPC/C complex (Apc1-300LΔ) was incubated with the indicated extracts lacking endogenous APC/C for 20 min, before addition of the *in vitro* translated FLAG-Cdc20-5A. All samples were analyzed by SDS-PAGE and immunoblotting using indicated antibodies. For binding assay to study interaction of APC/C with Apc1 fragments, purified Apc1 fragments were incubated with anti-FLAG Affinity M2 beads (Sigma-Aldrich) at 4°C for

1.5 h. Beads were washed with XB-CSF buffer and then incubated with interphase extract in the presence of Cyclin BΔ167 at 23°C for 1.5 h, separated from extract on Micro Bio-Spin columns (Bio-Rad), and washed twice with XB-CSF buffer containing 0.1% NP-40. The bound proteins were eluted with SDS-sample buffer and analyzed by SDS-PAGE and immunoblotting.

Cdc20 dissociation assay

The *in vitro* translated FLAG-Cdc20-5A or ^{35}S-labelled co-activators was added to MG132 supplemented CSF lacking Cdc20 (by immunodepletion) together with Apc3-beads at 23°C for 20 min to prepare the APC/C-Cdc20 complex. The resultant APC/C-Cdc20 complex was purified, washed once with XB-CSF buffer, and incubated in equal volume of indicated egg extracts or XB-CSF buffer at 23°C. Samples taken at the indicated time points were washed twice with XB-CSF containing 300 mM KCl and 0.01% NP-40 and eluted with SDS sample buffer, followed by analysis by SDS-PAGE and immunoblotting. For the preparation of rAPC/C-Cdc20 complex, purified rAPC/C was incubated with APC/C- and Cdc20-depleted CSF extract containing MG132 at 23°C for 60 min for proper phosphorylation, followed by a further 10–20 min incubation in the presence of *in vitro* translated FLAG-Cdc20-5A.

Cross-linking mass spectrometry

High Five cells were co-infected with both APC/C baculoviruses, cultivated at 27°C with shaking at 150 rpm for 48 h. To generate hyperphosphorylated APC/C, High Five cells were treated with 100 nM okadaic acid for 5 h prior to harvesting. The subsequent purification steps were performed at 4°C. Cell pellets were resuspended in APC/C lysis buffer [20 mM HEPES pH 7.9, 250 mM NaCl, 5% glycerol, 2 mM DTT, 0.5 mM EDTA, 10 μg/mL leupeptin, 10 μg/mL pepstatin A, 10 μg/mL chymostatin, and 30 units/mL benzonase (Novagen)]. The lysate was sonicated followed by centrifugation at 48,000x*g* for 60 min. The resulting supernatant was subjected to a second centrifugation for 20 min, and the final clarified supernatant was filtered through a 0.45 μm filter. The clarified supernatant was loaded onto a 5 mL Strep-Tactin Superflow Cartridge (Qiagen) at a flow rate of 0.5 mL/min. The column was washed with APC/C wash buffer (20 mM HEPES pH 7.9, 250 mM NaCl, 5% glycerol, and 2 mM DTT) at a flow rate of 1.5 mL/min. Recombinant APC/C was eluted using APC/C wash buffer supplemented with 2.5 mM desthiobiotin (Sigma-Aldrich). The fractions containing the peak protein were combined and concentrated using Amicon Ultra (Millipore). Cross-linking experiments of the unphosphorylated and hyperphosphorylated rAPC/C complexes were performed using bis(sulfosuccinimidyl)suberate (BS3, Thermo Fisher Scientific). Triplicate reactions of purified unphosphorylated (75 μg) or hyperphosphorylated (106 μg) rAPC/C complexes were incubated with BS3 (BS3:protein = 2:1 by weight) for 2 h on ice in 20 mM HEPES buffer (pH 7.9, 250 mM NaCl, 5% glycerol, 2 mM DTT, and 2.5 mM desthiobiotin). The cross-linking was stopped by the addition of 2.7 M ammonium bicarbonate stock. Cross-linking products were concentrated by a spin column (Amicon 100kDa cut off) and resolved using 4–12% NuPAGE (Invitrogen) for 30 min at 200 V and stained using Instant Blue (Expedeon). Cross-linked complex bands were excised, reduced, alkylated and trypsin digested following standard procedures.[47] Cross-linked peptides were desalted using C18 StageTips.[48]

Mass spectrometry

LC-MS/MS analysis for replicates was performed using Orbitrap Fusion Lumos (Thermo Fisher Scientific). The peptide separation was carried out on an EASY-Spray column (50 cm × 75 μm i.d., PepMap C18, 2 μm particles, 100 Å pore size, Thermo Fisher Scientific). Mobile phase A consisted of water and 0.1% formic acid. Mobile phase B consisted of 80% acetonitrile and 0.1% formic acid. Peptides were loaded onto the column with 2% B at 300 nL/min flow rate and eluted at 250 nL/min flow rate in two steps: linear increase from 2% B to 40% B in 109 or 139 min; then increase from 40% to 95% B in 11 min. The eluted peptides were directly sprayed into the mass spectrometer. Peptides were analyzed using a high/high strategy: both MS spectra and MS2 spectra were acquired in the Orbitrap. MS spectra were recorded at a resolution of 120,000. The ions with a precursor charge state between 3+ and 8+ were isolated with a window size of 1.6 m/z and fragmented using high-energy collision dissociation (HCD) with collision energy 30. The fragmentation spectra were recorded in the Orbitrap with a resolution of 15,000. Dynamic exclusion was enabled with single repeat count and 60 s exclusion duration.

The mass spectrometric raw files were processed into peak lists using ProteoWizard (version 3.0),[49] and cross-linked peptides were matched to spectra using xiSEARCH software (version 1.7.6.4) with preprocessing[50] and in-search assignment of monoisotopic peaks.[50] Search parameters were MS accuracy, 2 ppm; MS/MS accuracy, 6 ppm; enzyme, trypsin; cross-linker, BS3; max missed cleavages, 4; missing mono-isotopic peaks, 2; fixed modification, carbamidomethylation on cysteine; variable modifications, oxidation on methionine and phosphorylation on serine and threonine for phosphorylated sample; fragments, b and y ions with loss of H2O, NH3 and CH3SOH. The mass spectrometry proteomics data have been deposited to the ProteomeXchange Consortium via the PRIDE[51] partner repository with the dataset identifier ProteomeXchange: PXD050097 and PRoteomics IDEntifications (PRIDE) Database: PXD050097.

QUANTIFICATION AND STATISTICAL ANALYSIS

Quantification of gel images were performed using the ImageJ software, and information of each graph such as number of replicates and error bars can be found in their corresponding figure legends. All graphs were generated using Microsoft Excel.